Preprints of the 21st IFAC World Congress (Virtual)
Berlin, Germany, July 12-17, 2020

Image Reconstruction in Electrical Impedance Tomography via Artificial Neural Network in Two-Phase Flow

Koji Tanaka[1]. Yuya Takakura[2]. Prima Asmara Sejati[1].
Daisuke Kawashima[1]. Masahiro Takei[1].

[1]*Mechanical Engineering Course, Graduate School of Science and Engineering,*

Chiba University, Japan (e-mail: k_t19971022@chiba-u.jp).
[2]*Graduated from Mechanical Engineering Course, Graduate School of Science and*

Engineering, Chiba University, Japan (currently Panasonic Corporation)

(e-mail: xgkd3725@gmail.com)

Abstract: Electrical impedance tomography (EIT) technology is an image reconstruction technique based on the difference of electrical characteristics inside the measurement domain. The EIT is used in industrial applications such as gas distribution detection and mean gas void fraction estimation of two-phase flow in pipes. The most challenging in EIT is to solve nonlinear and ill-posed inverse problems. In the present study, the inverse problem is solved using an artificial neural network (ANN). ANN is trained using current vector $\boldsymbol{i}$ measured by voltage-current (VC) system. As a result, the proposed ANN shows a highly accurate image reconstruction as compared with the conventional method such as linear approximation and versatile applicability.

Keywords: Industrial applications of process control, Process control applications, Control of distributed systems, Image reconstruction, Neural Networks.

1. INTRODUCTION

Two-phase flow is generally common in various industrial equipment. A typical example is a flow in the core of a boiling water reactor, flow in the steam generator of pressurized water reactor, and flow in the evaporator tubes of thermal and industrial boilers. Imaging the fluid profile of two-phase flow in these industrial processes is essential for appropriate equipment control and safe equipment design in industrial plants as well as an in-depth analysis of fluid dynamics (Jeon, Do, Kawashima, and Takei, 2019).

As an imaging method, electrical impedance tomography (EIT) whose principal relies on taking advantage of the difference in the electrical properties of the two phases (Yorkey, Webster, and Tompkins, 1987) is proposed. In EIT, the current is injected into the measurement domain from electrodes in contact with the surface of the measurement domain, and voltage is measured (Liu, Jia, Zhang, and Yang, 2018). The image reconstruction in EIT consists of two problems: a forward problem and an inverse problem (Yao, and Takei, 2017). The forward problem means the calculation of voltage response under the boundary condition and the conductivity distribution in the measurement domain. The inverse problem means mapping of the cross-sectional conductivity distribution in the measurement domain based on the voltage. Since the inverse problem is nonlinear and ill-posed, it is challenging to obtain a unique optimal solution. Previously, the inverse problem is solved by linear approximation using a domain-specific sensitivity matrix, although, they only offer poor accuracy solutions at low speed. Furthermore, even slight noises contained in the measured voltage greatly affect the mapping of the cross-sectional conductivity distribution.

In order to solve the inverse problem with high accuracy, an artificial neural network (ANN) is proposed as an alternative method, which is suitable for processing nonlinear problems (Wang, G., 2016) and has high robustness and less affected by noises. However, few reports are available on the versatile applicability and spatial resolution of ANN. This present study evaluates the versatile applicability and spatial resolution of the proposed imaging method using EIT and ANN.

2. THEORY

2.1 VC system

A voltage injected and current measured (VC) system was developed by Henderson and Webster (Henderson, and Webster, 1978). Current vector $\boldsymbol{i}$ is measured by VC system as described in (Kim et al., 2014)

$$\boldsymbol{i} = \left[i_{1,2}, i_{1,3}, \cdots, i_{1,L}, i_{2,1} \cdots, i_{k,l}, \cdots, i_{K,L-1}\right] \\ \boldsymbol{i} \in \mathbb{R}_{K(L-1)},\ k \neq l \qquad (1)$$

where k (1, 2, ⋯, K) is the electrode number injected voltage, l (1, 2, ⋯, L) is the electrode number measured current, $i_{k,l}$ is the current scalar measured at the l^{th} electrode when the k^{th} electrode injected voltage v_k. Compared to the CV system commonly used in EIT (which measures voltage by injecting current), the VC system has the advantage of higher time resolution and simple hardware structure. Therefore, it is su

Table 1 Experimental condition

Electrode sensor diameter D_s	95.4 mm
Electrode diameter D_e	5.3 mm
Polyethylene rod diameter D_p	20 mm or 15 mm
Water conductivity σ_l	356.4 μS/cm
Polyethylene rod conductivity σ_p	10^{-14} μS/cm
Voltage magnitude v	1.0 V
Voltage frequency f	13 kHz

itable for observation of high-speed transient processes and useful for acquiring electrical characteristics of two-phase flow in industrial processes.

2.2 Proposed Artificial Neural Network Model

The forward propagation in the proposed ANN is composed of an input layer, a hidden layer consisting of three layers of M rectified linear units ReLUs (Hahnloser, Sarpeshkar, Mahowald, Douglas, Seung, 2000), and an output layer. Firstly, the current vector $\boldsymbol{i}$ is passed from the input layer to the hidden layer. Secondly, each ReLU creates an output scalar based on $\boldsymbol{i}$. Thirdly, M output scalars are passed to the output layer. Finally, the value of each image pixel is calculated by a linear function in the output layer. The backpropagation is performed using Nesterov accelerated adaptive moment estimation Nadam (Dozat, T., 2016). Furthermore, mini-batch training (Li, Zhang, Chen, and Smola, 2014), batch normalization (Ioffe, and Szegedy, 2015), early stopping (Prechelt, 1998), and dropout (Srivastava, Hinton, Krizhevsky, Sutskever, and Salakhutdinov, 2014) are used for the training efficiency improvement.

3. EXPERIMENT

In order to obtain the current vector $\boldsymbol{i}$, an electrode sensor with 8 electrodes was filled with liquid and one to three polyethylene rods were randomly arranged in it. As the train data in ANN, $\boldsymbol{i}$ was measured under 660 types of arrangement. As the test data, $\boldsymbol{i}$ was measured under different arrangements from that in train data. Also, $\boldsymbol{i}$ obtained under the arrangement of four polyethylene rods was measured in order to evaluate the versatile applicability of the proposed method. Table 1 shows experimental conditions in $\boldsymbol{i}$ measurement.

4. RESULTS

In addition to the proposed method, the inverse problem is solved using an algorism for linear approximation: one-step Gauss-Newton GN for comparison. Images from the one-step GN is binarized. Figure.1 shows the comparison of reconstructed images with one, two, and three polyethylene rods. Figure.1(a) shows true images. Figure.1(b) shows the reconstructed images using the one-step GN. Figure.1(c) shows the reconstructed images using the proposed ANN. For quantitative image accuracy evaluation, the structural similarity *SSIM* index (Wang, Bovik, Sheikh, and Simoncelli, 2004) between two image pixels **x, y** is calculated

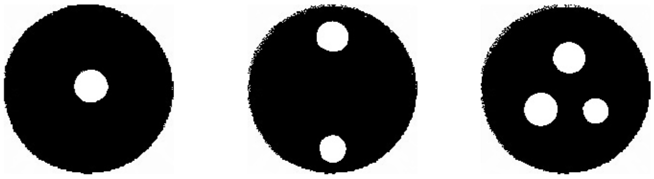

(a) True image

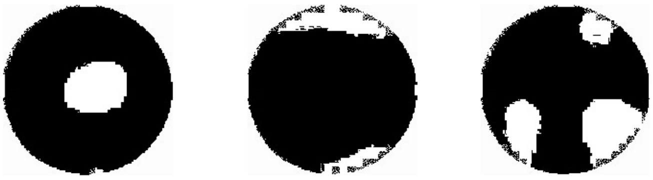

(b)One step GN

(c) Proposed ANN

Fig. 1. Comparison of reconstructed images.

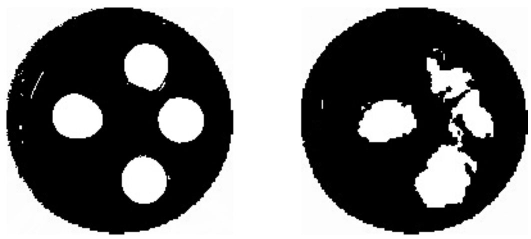

Fig. 2 Images at four polyethylene rods.

$$SSIM = \frac{(2\mu_x\mu_y+c_1)(2\sigma_{xy}+c_2)}{(\mu_x^2+\mu_y^2+c_1)(\sigma_x^2+\sigma_y^2+c_2)} \tag{2}$$

where μ is the average, σ is the variance, σ_{xy} is the covariance of **x** and **y**. c_1(= 6.5025) and c_2 (= 58.5225) are set by default. The average *SSIM* in Fig.1(b) and Fig.1(c) are 0.65 and 0.80, respectively. Figure 2 shows images at four polyethylene rods. The left side in Fig.2 is the true image and the right side is the reconstructed image by the proposed ANN. Although the train data does not include the current vector $\boldsymbol{i}$ under four polyethylene rods, it is qualitatively found that the position can be imaged even with four rods; namely, Image reconstruction using the proposed ANN has versatile applicability.

REFERENCES

Ioffe, S., and Szegedy, C. (2015). Batch normalization: Accelerating deep network training by reducing internal covariate shift. *arXiv preprint arXiv:1502.03167*.

Dozat, T. (2016). Incorporating nesterov momentum into adam. *International Conference on Learning Representations in Workshop (ICLRW)*, pp. 1-6, 2016.

Kim, B.S., Khambampati, A.K., Jang, Y.J., Kim, K.Y., and Kim, S. (2014). Image reconstruction using voltage-current system in electrical impedance tomography. *Nuclear Engineering and Design*, 278, pp.134-140.

Hahnloser, R. H., Sarpeshkar, R., Mahowald, M. A., Douglas, R. J., and Seung, H. S. (2000). Digital selection and analogue amplification coexist in a cortex-inspired silicon circuit. *Nature*, 405(6789), 947-951.

Henderson, R.P., and Webster, J.G. (1978). An impedance camera for spatially specific measurements of the thorax. *IEEE Transactions on Biomedical Engineering*, (3), pp.250-254.

Jeon, M., Do, M., Kawashima, D., and Takei, M. (2019). Application of Artificial Neural Network Model to a Voltage–Current System in the Estimation of Void-Fraction in a Gas-Liquid Flow. *IEEE Sensors Journal*, 19(13), pp.5098-5109.

Li, M., Zhang, T., Chen, Y., & Smola, A. J. (2014). Efficient mini-batch training for stochastic optimization. In *Proceedings of the 20th ACM SIGKDD international conference on Knowledge discovery and data mining,* pp. 661-670.

Liu, S., Jia, J., Zhang, Y. D., and Yang, Y. (2018). Image reconstruction in electrical impedance tomography based on structure-aware sparse Bayesian learning. *IEEE transactions on medical imaging*, 37(9), pp.2090-2102.

Prechelt, L. (1998). Automatic early stopping using cross validation: quantifying the criteria. *Neural Networks*, 11(4), 761-767.

Srivastava, N., Hinton, G., Krizhevsky, A., Sutskever, I., and Salakhutdinov, R. (2014). Dropout: a simple way to prevent neural networks from overfitting. *The journal of machine learning research*, 15(1), 1929-1958.

Yao, J., and Takei, M. (2017). Application of process tomography to multiphase flow measurement in industrial and biomedical fields: A review. *IEEE Sensors Journal*, 17(24), pp.8196-8205.

Yorkey, T.J., Webster, J.G., and Tompkins, W.J. (1987). Comparing reconstruction algorithms for electrical impedance tomography. *IEEE Transactions on Biomedical Engineering*, (11), pp.843-852.

Wang, G. (2016). A perspective on deep imaging. *IEEE Access*, 4, pp.8914-8924.

Wang, Z., Bovik, A. C., Sheikh, H. R., and Simoncelli, E. P. (2004). Image quality assessment: from error visibility to structural similarity. *IEEE transactions on image processing*, 13(4), 600-612.